Journal of Electroanalytical Chemistry 800 (2017) 25–31

Contents lists available at ScienceDirect

Journal of Electroanalytical Chemistry

journal homepage: www.elsevier.com/locate/jelechem

Simultaneous time-resolved ATR-SEIRAS and CO-charge displacement experiments: The dynamics of CO adsorption on polycrystalline Pt

Camila D. Silva [a], Gema Cabello [a], Wania A. Christinelli [a], Ernesto C. Pereira [a], Angel Cuesta [b,*]

[a] Departamento de Química, Universidade Federal de São Carlos, São Paulo, Brazil
[b] Department of Chemistry, University of Aberdeen, AB24 3UE, UK

ARTICLE INFO

Article history:
Received 18 July 2016
Received in revised form 29 September 2016
Accepted 17 October 2016
Available online 18 October 2016

Keywords:
Time-resolved ATR-SEIRAS
CO-charge displacement
Pt
CO adsorption

ABSTRACT

The high sensitivity of ATR-SEIRAS allowed simultaneous recording of time-resolved infrared spectra of the Pt-electrolyte interface and of the current flowing during CO-charge displacement experiments. These experiments revealed the dynamics of CO adsorption on Pt, as well as of the rearrangement of the interfacial water layer. Our experiments show that CO_L sites are populated first, CO_B appearing only at slightly higher coverages. At potentials sufficiently separated from the potential of zero total charge, the charge displaced upon CO adsorption on Pt and the integrated intensity of the CO_L band run approximately parallel, as also do the current transient and the time derivative of the integrated intensity of the CO_L band. This suggests that, for low to medium CO coverage, the current flowing at a given instant during the CO-charge displacement experiment corresponds to the instantaneous rate of CO adsorption, while the charge displaced when a CO submonolayer is formed is a good estimate of the corresponding relative coverage. Although the structure of the interfacial water layer is affected at low coverages, the band corresponding to interfacial water on top of a CO-covered Pt surface only appears at a relatively high CO coverage, suggesting that this kind of interfacial water is linked to the presence of compact islands of adsorbed CO.

1. Introduction

The development by Masatoshi Osawa of Surface Enhaced Infrared Absorption Spectroscopy in the Attenuated Total Reflection mode (ATR-SEIRAS) during the 1990s [1–3] has had a deep impact on our understanding of the structure of the electrode-electrolyte interface, and of the mechanism of electrocatalytic reactions. Compared to infrared reflection-absorbance spectroscopy (IRRAS), ATR-SEIRAS has the advantage of a higher sensitivity, and, due to the IRRAS requirement to work in a thin film configuration, also of unimpeded mass transport from the bulk of the electrolyte to the interface, and of comparably negligible uncompensated electrolyte resistance (R_u). Actually, the only advantage of IRRAS over ATR-SEIRAS is the possibility to work with single-crystal electrodes. The above-mentioned properties of ATR-SEIRAS enabled Osawa and co-workers to study the structure of water at the electrical double layer [4–6], to detect elusive intermediates in electrocatalytic reactions [7–10], to detect in real time changes in the electrode coverage by reaction intermediates during galvanostatic oscillations [11,12], to follow the dynamics of the rearrangement of the electrical double layer with ultra-high time resolution [13,14], to study the hydration shell of cations at the electrical double layer [15–17], to perform spectrokinetic studies of the mechanism of electrocatalytic reactions [18–20], etc.

The CO-charge displacement method was introduced by Clavilier and the Alicante group in the 1990′s, initially as a probe of the nature of the species present on the surface of a Pt electrode [21–23], but soon developed to a powerful method for the determination of the potential of zero total charge (pztc) of Pt single-crystal electrodes and other surfaces [24–27]. The method consists in the measurement of the current transient during adsorption of CO (dosed into the electrolyte close to the metal surface) at a controlled electrode potential. The charge obtained by integrating the current transient corresponds to the difference between the total charge density of the CO-covered Pt electrode and that of the initially CO-free Pt surface [26,27].

In sulphuric acid solutions, the surface of a Pt electrode is covered either by underpotential deposited hydrogen (H_{upd}) or by specifically adsorbed sulphate in the whole potential region relevant to CO-charge displacement experiments, and most of the charge flowing corresponds to the desorption of these specifically adsorbed species. However, during the potentiostatic adsorption of CO there will also be a change in the free charge density on the electrode surface, and a rearranging of the interfacial water layer, the former contributing to the current flowing, and both of them contributing to the potential profile across the interface. Similarly, not all the adsorption sites will be simultaneously populated by CO, and monitoring the sequence in which they are

* Corresponding author.
E-mail address: angel.cuestaciscar@abdn.ac.uk (A. Cuesta).

http://dx.doi.org/10.1016/j.jelechem.2016.10.034
1572-6657/

occupied can provide useful information regarding the kind of sites available, as well as on the relative energetics of the adsorption bond.

Here, we report time-resolved ATR-SEIRA spectra recorded simultaneously to CO-charge displacement experiments. These experiments allow to correlate the current flowing and the charge displaced with the increase in CO coverage, as well as to identify which adsorption sites are occupied first. They also allow monitoring in real time the rearrangement of the interfacial water layer.

2. Experimental

The working electrode was a thin platinum film deposited on one of the square faces of a triangular Si prism, bevelled at 60°, by the following chemical procedure. First, Pd was deposited on the Si substrate surface by contacting it with 0.5% HF containing 1 mM $PdCl_2$ for ca. 1.5 min in order to improve the adhesion of the Pt film to the substrate [28]. After rinsing with Milli-Q water, Pt was subsequently deposited on the Pd layer using a Pt plating bath. The plating bath was prepared as follows: (i) first, a solution 0.02 M in H_2PtCl_6 and 1 M in NH_3 was prepared, and left overnight in the fridge. This led to the formation of the $[Pt(NH_3)_6]^{4+}$ complex; (ii) 5 mL of this solution were diluted with 4.4 mL of ultrapure water, and 0.5 mL of concentrated NH_3 were added to the resulting mixture; (iii) finally, 0.1 mL of a 0.6 M solution of N_2H_4 were added to yield the final plating bath. Deposition was performed by covering the prism face with the plating bath at 60–70 °C for an appropriate period of time (typically 2–3 min). Pt films had a typical thickness of ca. 30 nm, as estimated from the value of the electrical resistance across the diagonal of the prism, and a roughness factor of 5.5. A typical cyclic voltammogram is shown in Fig. S1.

The Pt-covered Si prism was then attached to the spectroelectrochemical cell, using an O-ring to prevent electrolyte leakage. Electrical contact to the Pt film was achieved by pressing a circular Pt wire against it around the outside perimeter of the cell. Before the experiments, the Pt surface was electrochemically cleaned by repetitive cycling between 0 and 1.4 V vs. RHE in the supporting electrolyte (0.1 M H_2SO_4). A coiled Pt wire and a home-made reversible hydrogen electrode (RHE) were used as counter and reference electrodes, respectively.

ATR-SEIRA spectra were recorded in the Kretschmann configuration (internal reflection with a prism/metal film/solution geometry) with a Nicolet 6700 FTIR spectrometer equipped with an MCT detector, using *p*–polarized light. Unless otherwise indicated, each spectrum consisted of 5 interferograms, recorded with a spectral resolution of 8 cm^{-1} in the rapid-scan mode, with a time resolution of 0.69 s. The differential spectra were calculated as $-\log(R_{sample}/R_{reference})$, where $R_{reference}$ and R_{sample} are the reference and sample spectra, respectively. The reference spectrum consisted of 64 interferograms, and was recorded in the absence of CO just before each simultaneous CO-charge displacement/IR experiment, at the same potential at which the corresponding CO-charge displacement/IR experiment was to be performed.

The experiments were performed by simultaneously polarizing the Pt electrode at the desired potential and starting recording a spectral series. Then CO was bubbled through the solution, and the current transient and the evolution with time of the spectra were monitored simultaneously.

The working solutions were prepared from concentrated H_2SO_4 (Fluka Trace Select) and Milli-Q water. The solutions were deaerated with Nitrogen from a liquid nitrogen reservoir (99%, White Martins) before the experiments. CO-charge displacement experiments were performed by bubbling CO (99.25%, White Martins) through the solution at a constant potential.

3. Results and discussion

Experiments were performed at 0.10, 0.20, 0.30, and 0. 40 V. For the sake of clarity, only series of time-resolved spectra at 0.10 and 0.40 V, and only the first approximately 17 s after the onset of CO adsorption, are shown in Fig. 1. Similar series at 0.20 and 0.30 V are shown in the Supporting Information. Spectra corresponding to a saturated CO adlayer at each of these potentials, obtained by accumulating 64 interferograms at the end of the CO-charge displacement experiment, are shown in Fig. 2.

The bands that gradually appear in the spectra, and then start to increase, are easier to identify in Fig. 2: (i) a positive band around 3660 cm^{-1}, corresponding to the O—H stretching (ν(OH)) of interfacial water on the CO-covered Pt surface [6,29]; (ii) a very broad negative band with its maximum shifting from ca. 3490 cm^{-1} at 0.10 and 0.20 V to ca. 3530 cm^{-1} at 0.30 and 0.40 V, corresponding to ν(OH) of interfacial water on the CO-free Pt surface [6]; (iii) a positive band between 2068 and 2083 cm^{-1} (depending on both coverage and potential), corresponding to the C—O stretching of CO adsorbed linearly on Pt (CO_L); (iv) a positive and broad band around 1860 cm^{-1}, corresponding to the C—O stretching of CO bridge-bonded to the Pt surface (CO_B), which becomes more symmetric with increasing potential, in good agreement with previous work [30]; a positive band at ca. 1630 cm^{-1}, corresponding to the H-O-H bending (δ(HOH)) of interfacial water on CO-covered Pt [6]; and (v) a weak negative band around 1610 cm^{-1}, corresponding to δ(HOH) of interfacial water on bare Pt [6].

The only differences (in addition to the well-known blue shift of the CO stretching frequency with increasing potential) between the spectra at different potentials are (i) the presence of a negative band around 1200 cm^{-1}, corresponding to sulphate adsorbed on Pt [31], which is absent at 0.10 V, starts appearing at 0.20 V, and increases at 0.30 and 0.40 V; (ii) a blue shift of the negative ν(OH) band around 3500 cm^{-1} at 0.30 and 0.40 V, as compared to 0.10 and 0.20 V; and (iii) a decrease of the intensity of the negative δ(HOH) band around 1610 cm^{-1} with increasing potential. In the following, we will analyse these differences, as well as the dynamics of CO adsorption as deduced from the time evolution of the spectra in Fig. 1.

3.1. The dynamics of CO adsorption on Pt

It can be clearly seen from Fig. 1 that, at the very initial stages of CO adsorption, only on-top sites are occupied, CO_B appearing only later. This is in agreement with previous static IR spectra of low-coverage CO adlayers on stepped single-crystal electrodes, both in UHV [32–36] and in electrochemical environment [37–39], which consistently show CO_L appearing at lower coverage than CO_B, whose signal only emerges once the CO_L sites have been partially occupied.

A more detailed inspection of the time-resolved spectra in Fig. 1 reveals that, at the very initial stages of CO adsorption, during the first approximately 4 s, in addition to the main peak in the CO_L region, there is a second CO_L band at lower frequencies. This is illustrated in Fig. 3, again for the limiting cases of 0.10 and 0.40 V. In both cases, albeit slightly more clearly at 0.40 V, the main CO_L band, which peaks at 2068 and 2078 cm^{-1} at 0.10 and 0.40 V, respectively, is clearly accompanied by a smaller band, with peaks at approximately 2014 cm^{-1} (0.10 V, Fig. 3(A)) and 2025 cm^{-1} (0.40 V, Fig.3(B))). Despite its low intensity, the CO_B band also seems to have at least two components, around 1850 and 1800 cm^{-1} (with the low frequency tail extending further in the case of the spectra at 0.10 V, in good agreement with previous work [40]).

The lower frequency CO_L observed during these very initial stages of CO adsorption might be assigned to CO adsorbed on defect sites, while the higher frequency band could be attributed to CO adsorbed on terrace sites. However, several objections can be placed against this interpretation. First of all, a polycrystalline sample like the one used here can hardly be described as being composed of just steps and terraces. Polycrystalline Pt contains many (110)- and (100)-oriented step sites, as well as other defect sites like kinks and grain borders. It also contains some (111), and very few, if any, (100), terraces. Even more important than this, on stepped Pt single-crystal surfaces step sites are occupied first, both in UHV [32–36] and at electrochemical interfaces [37–39],

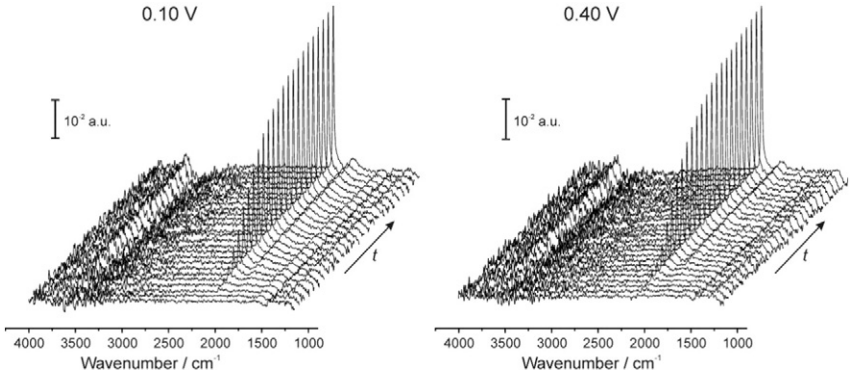

Fig. 1. Series of time-resolved ATR-SEIRA spectra recorded simultaneously to a *CO*-charge displacement experiment on a polycrystalline Pt electrode at 0.10 (left) and 0.40 V (right). Only the first approximately 17 s after the onset of CO adsorption are shown. The spectra are the result of accumulating 5 interferograms, with a time resolution of 0.69 s. The reference spectra, consisting of 64 interferograms, were those of a CO-free Pt electrode recorded just before the CO-charge displacement experiment at 0.10 (left) and 0.40 V (right).

terrace sites starting to be occupied only when there are no step sites available. On the contrary, in our experiments the CO_L band at higher frequencies appears first, and is always more intense than that at lower frequencies. Moreover, the frequency of the higher frequency CO_L band falls within the range typical for CO_L on Pt(111) electrodes, and shows a non-negligible degree of inhomogenous broadening even at the lowest coverages, suggesting that it involves several adsorption sites absorbing at similar frequencies. CO_L adsorbed on (100) terraces appears at frequencies clearly lower than those corresponding to (111) terraces (2053–2061 cm^{-1} for CO_L on Pt(100) [41], as opposed to 2066–2077 cm^{-1} for CO_L on Pt(111) [42]). If the (100) sites present on the polycrystalline Pt surface are mainly step sites, the corresponding CO_L frequency would be even lower. Consequently, an alternative interpretation for the spectra at very low coverage in Fig. 3 is that the band at higher frequencies corresponds to CO_L adsorbed on (110)-oriented defects (typically observed around 2070 cm^{-1} [43]) and (111) terraces, while the band at lower frequencies corresponds to CO_L adsorbed on (100)-oriented sites (mainly defects).

Similarly, the two components of the band just above 1800 cm^{-1} can also be attributed to CO_B at terraces and steps. These two components can be observed even at high coverage, which has been attributed to the lower coverage, and consequently lower degree of dipole-dipole coupling, of CO_B [30]. The low-frequency component appears at a frequency characteristic of CO_B on (100)-oriented step sites [14,19,40]. However, the CO_B band in the spectra of the complete adlayer becomes

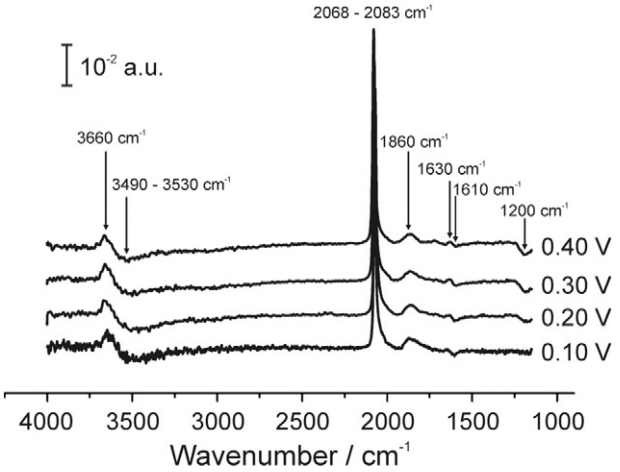

Fig. 2. ATR-SEIRA spectra of the saturated CO adlayer on a polycrystalline Pt electrode at 0.10, 0.20, 0.30, and 0.40 V, recorded just after the CO-charge displacement experiment. The spectra were obtained by accumulating 64 interferograms. The reference spectra, also consisting of 64 interferograms, were those of a CO-free Pt electrode recorded just before the CO-charge displacement experiment at the corresponding potential.

sharper and clearly more symmetric as the potential increases (Fig. 2). This is similar to the behaviour of CO_B on Pt(111) electrodes, and has been shown to be triggered by a small decrease in the CO coverage [42]. This suggests that there is also some contribution to the low-frequency part of the CO_B band at 0.10 V from CO_B on (111) terraces.

It can also be observed in Figs. 3(C) and (D) that the frequency of the peak at higher frequencies remains constant with increasing coverage during the initial stages of the experiment. A slight blue shift appears only in the spectrum at the longest time in Fig. 3 (C). The stretching frequency of chemisorbed CO is known to be strongly coverage dependent, due to dipole-dipole coupling between neighbouring oscillating dipoles with slightly different oscillation frequencies. Dipole-dipole coupling causes dipoles oscillating at the same or very similar frequencies to couple their phases, thereby increasing their oscillation frequency, and making dipoles at lower frequency lose intensity in favour of those appearing at higher frequency (a phenomenon called intensity borrowing) [44]. As can be seen in Fig. 3 (compare the spectrum at 3.45 s in Fig. 3(C) with those at earlier times, or the spectra at very low coverage in both Fig. 3(C) and (D), with those at the end of the series, once the CO-charge displacement experiment has been completed), once the coverage has increased sufficiently, dipole-dipole coupling leads to an increase in the frequency of the main CO_L band, while that at lower frequency merges with the higher frequency one, contributing to its inhomogeneous broadening. The constant frequency of the main CO_L band at the very initial stages of the adsorption process corroborates that the spectra in Fig. 3 correspond to isolated CO islands with low coverage dispersed over the Pt surface. The observed increase in intensity of the CO_L band without a concomitant blue shift of its stretching frequency suggests that, initially, the number of these islands increases with increasing CO coverage, but the local coverage within them remains constant.

Another interesting observation worth discussing here refers to the difference between the very low coverage adlayers observed in our experiments during the initial stages of the CO adsorption process and those formed in the final stages of the electrooxidation of adsorbed CO [40]. In their time-resolved study of the dynamics of the electrooxidation of the CO adlayer, Samjeské et al. [40] found that, in the final stages of the stripping process, the last CO molecules remaining on the surface before complete oxidation of the adlayer are CO_B at defect sites. This is intriguing, because the results shown here, as well as in previous work with single-crystal electrodes [32–39], clearly indicate that, at low coverage, CO_L is favoured over CO_B, both on defects and terraces. Accordingly, it would be expected that, upon oxidation of a considerable amount of the CO adlayer, when the coverage has decreased and reached a value similar to that corresponding to the spectra in Fig. 3, CO_B, whether on defects or on terraces, would convert to CO_L. It might be argued that the difference between Samjeské's et al. results during CO stripping and our observations during CO adlayer formation are

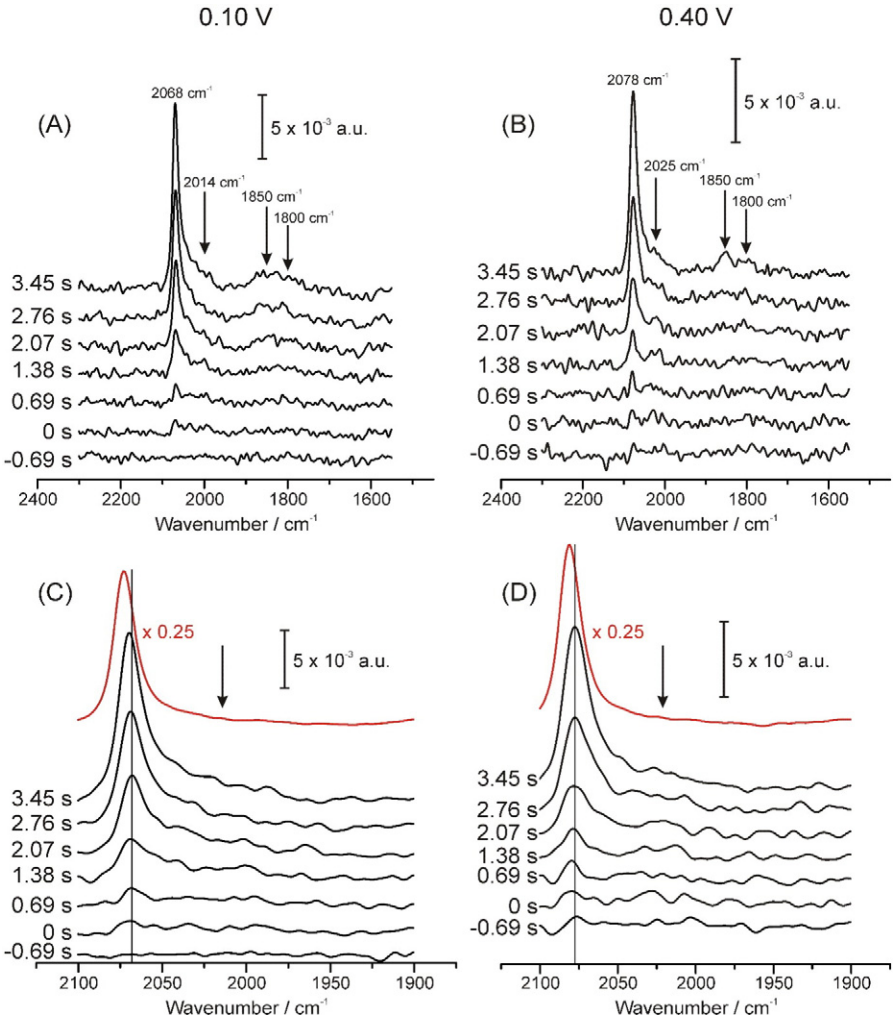

Fig. 3. Selected ATR-SEIRA spectra in the spectral region corresponding to the C—O stretching band of adsorbed CO extracted from those in Fig. 1 and corresponding to the first 4 s of the CO-charge displacement experiment at 0.10 V (A and C) and 0.40 V (B and D). The vertical arrows indicate the position of the low-frequency CO_L band appearing at very low CO coverage. The vertical line in C and D indicates the peak frequency of the CO_L band at very low CO coverage. The red line corresponds to the spectrum of a complete CO adlayer, obtained after the CO-charge displacement experiment.

related to the different potentials at which the experiments were performed (between 0.10 and 0.40 V in our case, between 0.70 and 0.80 V in [40]), but it is well known that CO_B is favoured at negative potentials. This discrepancy might be explained, though, if it is assumed that CO_B must convert to CO_L before the Langmuir-Hinshelwood reaction with adsorbed OH (OH_{ad}) can take place, and if the potential dependence of the two successive reactions (CO site conversion and CO oxidation) involved in the final stages of the CO stripping process is considered. The oxidation of the last CO_B molecules remaining on the surface of the Pt electrode must follow, accordingly, the following mechanism:

$$CO_B \overset{k_{s.c.}}{\rightarrow} CO_L \tag{1}$$

$$CO_L + OH_{ad} \overset{k_{L-H}}{\rightarrow} CO_2 + H^+ + e^- \tag{2}$$

where $k_{s.c.}$ is the rate constant for the site-conversion process from CO_B to CO_L, and $k_{L\text{-}H}$ is the rate constant for the Langmuir-Hinshelwood reaction between CO_L and OH_{ad}. The rate at which CO_L forms will be given by:

$$\frac{d\theta_{CO_L}}{dt} = k_{s.c.}\theta_{CO_B} - k_{L-H}\theta_{OH}\theta_{CO_L} \tag{3}$$

Both $k_{L\text{-}H}$ and θ_{OH} increase with increasing potential, while $k_{s.c}$ can be expected to depend very weakly, if at all, on the electrode potential. Consequently, at positive enough potentials the rate of the Langmuir-Hinshelwood reaction between CO_L and OH_{ad} will be much faster than the rate at which CO_B converts to CO_L. In this scenario, CO_L will oxidise instantaneously after the site conversion and will not be observed in the final stages of the CO stripping process, in good agreement with Samjeské et al. [40]. If this hypothesis is correct, a dynamic ATR-SEIRAS experiment, in which the potential is pulsed back to 0.10 or 0.20 V after nearly complete oxidation of the CO adlayer, should show the conversion of the remaining CO_B into CO_L. This experiment, however, falls out of the scope of the present work, and will be reported elsewhere.

3.2. Correlation between the potentiostatic current and CO-coverage transients

Fig. 4 shows plots of the current transients during the CO-charge displacement experiments and of the time derivative of the integrated intensity of the CO_L band ($\frac{dI_{CO}}{dt}$) vs. time (Figs. 4(A) and (C)), as well as of the charge transferred and the integrated intensity of the CO_L band (I_{CO}) as a function of time (Figs. 4(B) and (D)), at 0.10 and 0.40 V. We restrict ourselves to these potentials, which are far enough from the pztc as to yield completely positive (0.10 V) or completely negative

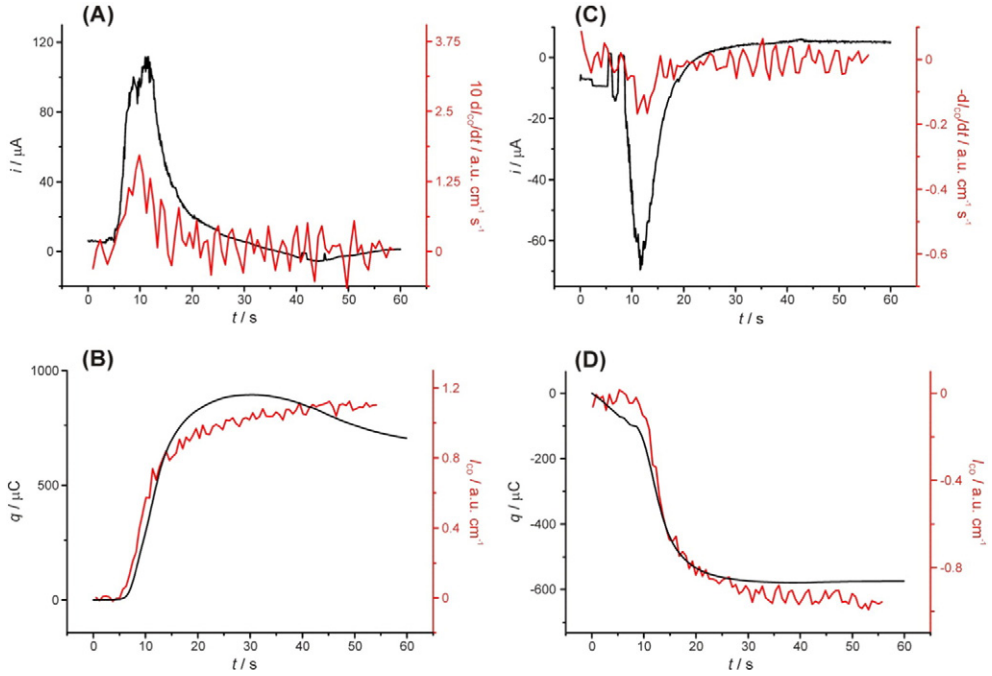

Fig. 4. (A) and (C): Correlation between the current transient during a CO-charge displacement experiment (black line) and the derivative of the integrated intensity of the CO_L band in simultaneous time-resolved ATR-SEIRA spectra (red line); (B) and (D): Correlation between the surface charge, obtained by integration of the current transient, and the integrated intensity of the CO_L band in simultaneous time-resolved ATR-SEIRA spectra (B and D). The experiments were performed at 0.10 V (A and B) and 0.40 V (C and D).

(0.40 V) current transient. At potentials close to the pztc bipolar transients can appear, which makes their analyses in terms of simultaneously recorded ATR-SEIRA spectra more complicated.

At coverage low enough, when dipole-dipole interactions still have little influence on the intensity of IR absorption by adsorbed CO, the integrated intensity of CO_L has been shown to be proportional to CO coverage (θ_{CO}). Accordingly, at least at the initial stages of the experiment, just before the maximum in the current transient, a plot of I_{CO} vs. t shows the gradual increase in θ_{CO}, while a plot of $\frac{dI_{CO}}{dt}$ vs. t is equivalent to a plot of the rate of CO adsorption as a function of time. Interestingly, Figs. 4(A) and (C) clearly show that, at least at times before the current transient maximum, the current transient runs parallel to the $\frac{dI_{CO}}{dt}$ vs. t plot, suggesting that the current flowing at every instant during the CO-charge displacement experiment is a direct measure of the instantaneous rate of CO adsorption. This rate increases initially as the concentration of CO near the surface increases once CO bubbling has started, reaching a maximum and starting to decreases when θ_{CO} is high. This suggests that the adsorption process itself is fast, being limited by the transport of CO molecules to the electrode surface at low coverage, and by the availability of adsorption sites at high coverage.

Similarly, the curve obtained after integration of the current transient, which corresponds to the charge flown from the beginning of the CO-charge displacement up to a given time, runs, at least at times shorter than the current maximum, parallel to the I_{CO} vs. t, suggesting that the charge flown at any moment during the CO-charge displacement experiment is a direct measure of the relative CO coverage ($\frac{\theta_{CO}}{\theta_{CO}^{max}}$) achieved up to that instant.

CO-charge displacement transients are very sensitive to the presence of contaminants, and quantitatively reliable results can only be obtained in ultra-clean conditions. These conditions are difficult to achieve in ATR-SEIRAS experiments, partly due to the very likely presence of residues from the plating solution on the Pt surface, and in the present case are affected by the relatively low purity of the CO used. The charge density (per real surface area) obtained upon integration of the transient at 0.1 V (ca. 100 μC cm^{-2}) is clearly lower than typically found with Pt(poly) in ultraclean conditions (170 μC cm^{-2}) [30]. On the contrary, the charge density obtained upon integration of the transient at 0.5 V (ca. -63 μC cm^{-2}) is clearly higher than typically found with Pt(poly) in ultraclean conditions (−32 μC cm^{-2}) [30]. We attribute this to a negative contribution from the reduction of oxygen present in the commercial CO gas used.

3.3. Changes in the structure of interfacial water during the CO adsorption process

The spectra of the complete CO adlayer in Fig. 2 show one positive and one negative absorption band in the region of the O—H stretching mode of water (ν(OH), above 2500 cm^{-1}), as well as one positive and one negative absorption band in the region of the H-O-H bending mode of water (δ(HOH), between 1550 and 1670 cm^{-1}). The negative-going bands correspond to interfacial water adsorbed on the Pt surface before CO adsorption, while the positive-going bands correspond to interfacial water adsorbed on the CO-covered Pt surface. These spectral features are consistent with those previously reported by Osawa et al. [6]. Slight differences arise due to the choice of different reference and sample potentials in [6] and in the work reported here.

For the interpretation of the negative-going bands, i.e., of the spectrum of interfacial water on CO-free Pt, we follow Osawa et al. [6]. Briefly, the negative band around 3550 cm^{-1} in the spectra at 0.10 and 0.20 V appears at a frequency clearly higher than that typical of bulk water (3400 cm^{-1} [45]), suggesting a lower degree of hydrogen bonding at the Pt-electrolyte interface as compared with the bulk. The red shift of the negative-going δ(HOH) band (around 1611 cm^{-1}), as compared with that typical of bulk water (1645 cm^{-1}) is also consistent with a lower degree of hydrogen bonding (hydrogen bonding typically results in a blue shift of the δ(HOH) band), although the observed red shift is larger than that expected exclusively from a decrease in hydrogen bonding (see [6] and discussion below). According to Osawa et al., this spectrum corresponds to a first layer of water molecules slightly tilted with their two hydrogen atoms pointing towards the surface, but not vertically. This prevents hydrogen bonding among the first-

layer water molecules, but allows the interaction of one of the oxygen lone pairs with the Pt surface (explaining the very low δ(HOH) frequency [46]), while the other one can act as a hydrogen acceptor and form hydrogen bonds to water molecules in the second layer (explaining the high frequency of the ν(OH) band, which is less perturbed in hydrogen acceptors than in hydrogen donors [47]).

The negative-going δ(HOH) band is weaker at 0.30 and, particularly, 0.40 V. This is consistent with the molecules in the first water layer gradually orienting their dipole parallel to the Pt surface, and then reorienting with their hydrogen atoms pointing to the solution, as the potential approaches, and then goes over, the pzc (around 0.30 V [30]). This reorientation will favour hydrogen bonding among interfacial water molecules, which agrees with the emergence of a weak and very broad band centred at 3000 cm^{-1} at 0.30 and 0.40 V, characteristic of very strongly hydrogen bonded ice-like water molecules [45,46,48]. The blue shift of the ν(OH) band in Fig. 2 has been attributed by Osawa et al. [6] to a new band due to the disruption of the ice-like water structure by adsorbed sulphate, leading to almost free OH bonds in the water molecules surrounding the adsorbed anions. This interpretation is supported by the fact that the changes in the ν(OH) spectral feature are accompanied by the emergence of a band around 1200 cm^{-1} characteristic of adsorbed sulphate.

Regarding the structure of the water layer on the CO-covered Pt surface, it is characterised by a sharp ν(OH) band at 3660 cm^{-1} and a δ(HOH) band at 1630 cm^{-1}. The latter can be better appreciated in the spectra at 0.30 and 0.40 V due to less interference from the weaker negative absorption band of the δ(HOH) mode of water adsorbed on CO-free Pt. These bands are typical of water free of hydrogen bonding, suggesting a very weak interaction of the first water layer both with the CO adlayer on the Pt surface and with water molecules in the second layer. Taking into account the negative (free) charge density present on the surface of a CO-covered Pt electrode [27], these water molecules must be oriented with their hydrogen atoms pointing to the metal surface. An interesting observation is that the intensity and position of both the ν(OH) and δ(HOH) bands of water adsorbed on the CO-covered Pt surface do not seem to be affected by the electrode potential. This suggests that, at (free) charge densities characteristic of CO-covered Pt in the potential region between 0.10 and 0.40 V (between ca. −16 and −10 μC cm^{-2} [27]) dielectric saturation of the interfacial water layer on CO-covered Pt has been attained.

The dynamic nature of our experiments allows us to go beyond the analysis of the structure of the interfacial water layer, and to analyse, at each potential, the evolution from the structure characteristic of a clean Pt surface to that typical of a CO-covered Pt electrode. Fig. 5 shows selected spectra recorded during the first 18 s of the CO adsorption process (as in Fig. 3, $t = 0$ was taken as the instant at which a signal for CO_L can be first observed in the ATR-SEIRA spectral series). Only results at 0.40 V are shown because, due to the low intensity of the δ(HOH) band of water adsorbed on the initially CO-free Pt surface (see discussion above), the δ(HOH) band of water adsorbed on the CO-covered Pt electrode is less distorted, and is easier to analyse.

A weak negative band around 3550 cm^{-1} starts to appear as soon as adsorbed CO is detected in the ATR-SEIRA spectra, as illustrated by the spectra at 2.4 and 4.8 s after the beginning of CO adsorption in Fig. 5. No positive band indicative of water molecules rearranging in a different structure can be observed, suggesting that, at these extremely low CO coverage, this band is simply due to the decrease in the coverage of the corresponding water species, namely, water adsorbed on bare Pt. The positive sharp ν(OH) band around 3660 cm^{-1} appears only when the CO coverage has increased considerably, and is accompanied by the emergence of the positive δ(HOH) band around 1630 cm^{-1} (see spectra at 6.87 and 8.94 s in Fig. 5). The emergence of these bands coincides with a blue shift of the CO_L band, attributed to dipole-dipole coupling between CO oscillators on the Pt surface. This implies that a relatively high coverage by CO is necessary for the interfacial water layer to adopt the structure typical of water adsorbed on CO-covered Pt.

4. Conclusions

The high sensitivity characteristic of ATR-SEIRAS allows obtaining a good enough signal-to-noise ratio without the need to accumulate a large number of interferograms. This, together with the absence of transport limitations, allows registering spectral series with a time resolution high enough to monitor, in real time, the CO adsorption process while simultaneously recording the CO-charge displacement current

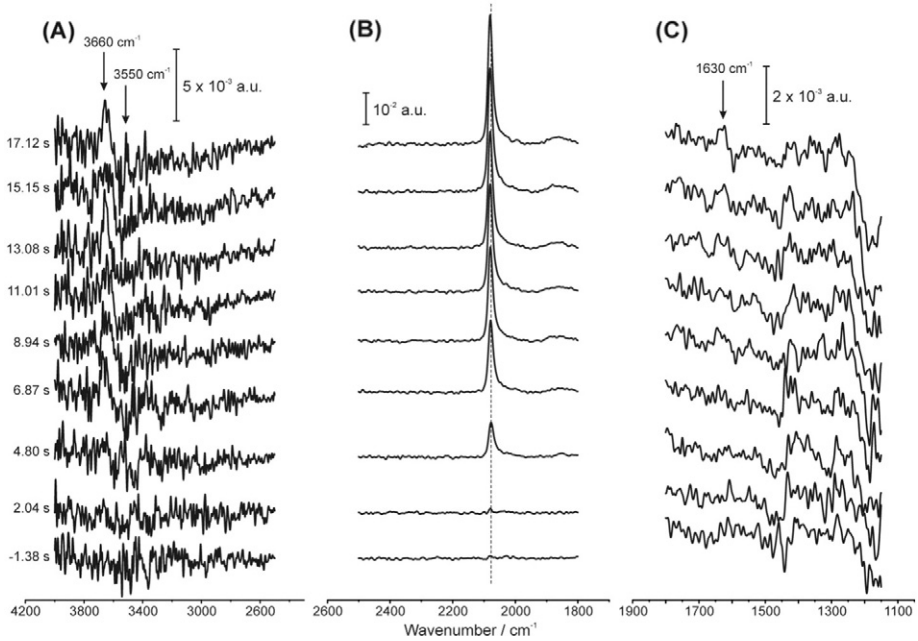

Fig. 5. ATR-SEIRA spectra selected among those recorded during the first 17 s of the CO-charge displacement experiment at 0.40 V, extracted for those presented in Fig. 1. The spectral regions corresponding to the ν(OH) and δ(HOH) modes of water are shown in an expanded scale for better identification of the corresponding bands. The vertical dashed line in the central panel corresponds to the peak frequency of the CO_L band at very low CO coverage. The arrows in the left and right panels indicate the position of the ν(OH) and δ(HOH) bands, respectively, of water adsorbed on top of the CO adlayer on Pt.

transient. These experiments have revealed that CO_L are preferred to CO_B sites, and are occupied first. Furthermore, during the initial stages of CO adsorption, when CO coverage is very low, two bands corresponding to CO_L could be resolved, due to the absence of dipole-dipole coupling between CO molecules at different sites at this low coverage. Although these two bands could be assigned to CO_L adsorbed at steps (lower frequency CO_L band) and terraces (higher frequency CO_L band), due to the polycrystalline nature of our sample, and to the observation that both bands appear simultaneously, we believe that assigning them to (100)-like defect sites (lower frequency CO_L band) and (110)-like defect + (111) terrace sites (higher frequency CO_L band) is more reasonable. The presence of multiple CO_B sites is also evident from the broad nature of the CO_B band, but, due to its low intensity, discrete bands cannot be resolved. The simultaneous recording of ATR-SEIRA spectra and of the current transients during CO adsorption has allowed us to show that, at least at times shorter than the current maximum in the transient (and at potentials negative enough or positive enough from the pztc, where completely positive or negative current transients, respectively, are obtained), the current flowing at every instant is a direct measure of the rate of CO adsorption, while the charge displaced up to that instant corresponds to the CO coverage reached. Finally, an analysis of the evolution of the bands in the regions of the ν(OH) and δ(HOH) vibrational modes of water reveals that, although the coverage of interfacial water with a structure characteristic of water adsorbed on bare Pt starts to decrease as soon as CO starts adsorbing on Pt, the structure typical of water adsorbed on CO-covered Pt only appears when a relatively high CO coverage has been reached. This suggests that formation of the essentially hydrogen bond-free water layer characteristic of water adsorbed on the CO adlayer on Pt requires relatively compact CO islands.

Acknowledgement

The support of FAPESP (Project No 2013/07296-2) and of the University of Aberdeen is gratefully acknowledged. AC thanks CAPES for a PVE grant (Project No A090/2013). GC gratefully acknowledges the support of CNPq through Research Project BJT-2014/400117/2014-2.

Appendix A. Supplementary data

Supplementary data to this article can be found online at doi:10.1016/j.jelechem.2016.10.034.

References

[1] M. Osawa, K.-i. Ataka, Surf. Sci. 262 (1992) L118.
[2] M. Osawa, K.-I. Ataka, K. Yoshii, Y. Nishikawa, Appl. Spectrosc. 47 (1993) 1497.
[3] M. Osawa, K.-i. Ataka, K. Yoshii, T. Yotsuyanagi, J. Electron Spectrosc. Relat. Phenom. 64–65 (1993) 371.
[4] K.-i. Ataka, T. Yotsuyanagi, M. Osawa, J. Phys. Chem. 100 (1996) 10664.
[5] K.-i. Ataka, M. Osawa, Langmuir 14 (1998) 951.
[6] M. Osawa, M. Tsushima, H. Mogami, G. Samjeske, A. Yamakata, J. Phys. Chem. C 112 (2008) 4248.
[7] Y.X. Chen, A. Miki, S. Ye, H. Sakai, M. Osawa, J. Am. Chem. Soc. 125 (2003) 3680.
[8] A. Miki, S. Ye, T. Senzaki, M. Osawa, J. Electroanal. Chem. 563 (2004) 23.
[9] K. Kunimatsu, T. Senzaki, M. Tsushima, M. Osawa, Chem. Phys. Lett. 401 (2005) 451.
[10] M. Osawa, K.-i. Komatsu, G. Samjeské, T. Uchida, T. Ikeshoji, A. Cuesta, C. Gutiérrez, Angew. Chem. Int. Ed. 50 (2011) 1159.
[11] Y. Mukouyama, M. Kikuchi, G. Samjeské, M. Osawa, H. Okamoto, J. Phys. Chem. B 110 (2006) 11912.
[12] G. Samjeské, A. Miki, M. Osawa, J. Phys. Chem. C 111 (2007) 15074.
[13] A. Yamakata, T. Uchida, J. Kubota, M. Osawa, J. Phys. Chem. B 110 (2006) 6423.
[14] A. Yamakata, M. Osawa, J. Phys. Chem. C 112 (2008) 11427.
[15] A. Yamakata, M. Osawa, J. Am. Chem. Soc. 131 (2009) 6892.
[16] A. Yamakata, M. Osawa, J. Phys. Chem. Lett. 1 (2010) 1487.
[17] A. Yamakata, E. Soeta, T. Ishiyama, M. Osawa, A. Morita, J. Am. Chem. Soc. 135 (2013) 15033.
[18] A. Cuesta, G. Cabello, C. Gutierrez, M. Osawa, Phys. Chem. Chem. Phys. 13 (2011) 20091.
[19] A. Cuesta, G. Cabello, M. Osawa, C. Gutiérrez, ACS Catal. 2 (2012) 728.
[20] A. Cuesta, G. Cabello, F.W. Hartl, M. Escudero-Escribano, C. Vaz-Domínguez, L.A. Kibler, M. Osawa, C. Gutiérrez, Catal. Today 202 (2013) 79.
[21] J. Clavilier, R. Albalat, R. Gomez, J.M. Orts, J.M. Feliu, A. Aldaz, J. Electroanal. Chem. 330 (1992) 489.
[22] J.M. Orts, R. Gómez, J.M. Feliu, A. Aldaz, J. Clavilier, Electrochim. Acta 39 (1994) 1519.
[23] J.M. Orts, R. Gómez, J.M. Feliu, A. Aldaz, J. Clavilier, Langmuir 13 (1997) 3016.
[24] E. Herrero, J.M. Feliu, A. Wieckowski, J. Clavilier, Surf. Sci. 325 (1995) 131.
[25] R. Gómez, V. Climent, J.M. Feliu, M.J. Weaver, J. Phys. Chem. B 104 (1999) 597.
[26] M.J. Weaver, Langmuir 14 (1998) 3932.
[27] A. Cuesta, Surf. Sci. 572 (2004) 11.
[28] S. Karmalkar, J. Banerjee, J. Electrochem. Soc. 146 (1999) 580.
[29] A. Cuesta, J. Electroanal. Chem. 587 (2006) 329.
[30] A. Cuesta, A. Couto, A. Rincón, M.C. Pérez, A. López-Cudero, C. Gutiérrez, J. Electroanal. Chem. 586 (2006) 184.
[31] K. Kunimatsu, M.G. Samant, H. Seki, M.R. Philpott, J. Electroanal. Chem. 243 (1988) 203.
[32] B.E. Hayden, K. Kretzschmar, A.M. Bradshaw, R.G. Greenler, Surf. Sci. 149 (1985) 394.
[33] F.M. Leibsle, R.S. Sorbello, R.G. Greenler, Surf. Sci. 179 (1987) 101.
[34] J. Xu, P. Henriksen, J.T. Yates, J. Chem. Phys. 97 (1992) 5250.
[35] J. Xu, J.T. Yates, J. Chem. Phys. 99 (1993) 725.
[36] J.T. Yates, J. Vac. Sci. Technol. A 13 (1995) 1359.
[37] C.S. Kim, C. Korzeniewski, Anal. Chem. 69 (1997) 2349.
[38] C.S. Kim, C. Korzeniewski, W.J. Tornquist, J. Chem. Phys. 100 (1994) 628.
[39] C.S. Kim, W.J. Tornquist, C. Korzeniewski, J. Phys. Chem. 97 (1993) 6484.
[40] G. Samjeské, K.-i. Komatsu, M. Osawa, J. Phys. Chem. C 113 (2009) 10222.
[41] A. López-Cudero, Á. Cuesta, C. Gutiérrez, J. Electroanal. Chem. 586 (2006) 204.
[42] A. López-Cudero, A. Cuesta, C. Gutiérrez, J. Electroanal. Chem. 579 (2005) 1.
[43] S.-C. Chang, M.J. Weaver, Surf. Sci. 230 (1990) 222.
[44] F.M. Hoffmann, Surf. Sci. Rep. 3 (1983) 107.
[45] G.L. Richmond, Chem. Rev. 102 (2002) 2693.
[46] P.A. Thiel, T.E. Madey, Surf. Sci. Rep. 7 (1987) 211.
[47] B.M. Auer, J.L. Skinner, Chem. Phys. Lett. 470 (2009) 13.
[48] M.A. Henderson, Surf. Sci. Rep. 46 (2002) 1.